Materials Horizons

ROYAL SOCIETY OF CHEMISTRY

COMMUNICATION

View Article Online
View Journal | View Issue

Cite this: *Mater. Horiz.*, 2025, **12**, 5762

Received 5th March 2025,
Accepted 7th May 2025

DOI: 10.1039/d5mh00397k

rsc.li/materials-horizons

Humidity-driven modulation of ferroelectricity in hafnia–zirconia membranes†

Haoze Zhang, ‡[ab] Yufan Shen, ‡[c] Pankaj Sharma, [ade] Lei Wang, [b] Dawei Zhang, [bd] Kousuke Ooe, [f] Shunsuke Kobayashi, [f] Yuichi Shimakawa, [c] Daisuke Kan *[c] and Jan Seidel *[bd]

Ferroelectric hafnia-based compounds, known for exhibiting strong ferroelectricity in films of sub-5 nm thickness, hold significant potential for being integrated into complementary metal-oxide-semiconductor devices. Due to the polymorphic nature of hafnia, their ferroelectric properties can be modulated through various mechanisms, including defects, strain, and electrochemical states. In this study, we fabricated ultrathin freestanding hafnia membranes, free from substrate and electrode-capping effects, to explore the relationship between their intrinsic ferroelectricity and surface electrochemical state by modulating humidity conditions during scanning probe microscopy measurements. Our results demonstrate enhanced ferroelectricity in hafnia under low-humidity conditions without requiring a wake-up process. This enhancement is attributed to reduced adsorption of water molecules on the membrane surface, which helps preserve oxygen vacancies that stabilize the ferroelectric phase in hafnia under an applied electric field. These findings suggest that beyond electrical control *via* field-cycling-induced phase transitions, electrochemical modulation through humidity provides an effective approach for tuning the ferroelectric properties of hafnia-based compounds, optimizing their performance in flexible nanoelectronics applications.

New concepts

In this manuscript, we present a novel strategy for enhancing ferroelectricity in freestanding hafnia membranes by controlling ambient humidity, demonstrating that low-humidity conditions significantly improve ferroelectric properties without requiring a wake-up process. This enhancement is attributed to the reduced adsorption of water molecules, which helps preserve oxygen vacancies crucial for stabilizing the ferroelectric phase in hafnia. Unlike previous studies, which were influenced by substrate, electrode-capping effects, or minimal surface contributions due to large film thicknesses, we fabricated ultrathin freestanding hafnia membranes completely free from these constraints. By varying humidity conditions during scanning probe microscopy measurements, we investigated the intrinsic relationship between ferroelectricity and the surface electrochemical state. This work introduces electrochemical modulation *via* humidity as a novel alternative to conventional field-cycling methods for tuning hafnia-based ferroelectrics, paving the way for improved performance in flexible nanoelectronic devices.

Introduction

Ferroelectricity in fluorite-structure oxides, *e.g.* hafnia and zirconia, was first reported by Böscke *et al.*,[1,2] marking the initial reliable observation of polarization in a binary oxide. In contrast to traditional single-crystal ferroelectric ABO_3 perovskites, hafnium-based thin films can display robust ferroelectricity with polycrystallinity fabricated by atomic layer deposition or sputtering, being compatible with modern semiconductor manufacturing workflows. This capability paves the way for large-scale applications of ferroelectric non-volatile random-access memories (FeRAM),[3,4] energy harvesters,[5,6] electrostatic supercapacitors,[7,8] ferroelectric field-effect transistors (FeFETs)[9–12] and ferroelectric tunnel junctions (FTJ).[13–16] Additionally, this discovery has spurred interest in alternative emerging polar materials, such as $Al_xSc_{1-x}N$[17] and $Mg_xZn_{1-x}O$.[18–21]

Hafnia-based thin films exhibit more complex ferroelectric behavior than traditional ferroelectrics due to their polymorphic nature, which involves the coexistence of stable and metastable phases.[22–24] The switchable polarisation in hafnia is

[a] College of Science and Engineering, Flinders Microscopy and Microanalysis, Flinders University, Bedford Park, Adelaide, SA, 5042, Australia
[b] School of Materials Science and Engineering, UNSW Sydney, Sydney 2052, Australia. E-mail: jan.seidel@unsw.edu.au
[c] Institute for Chemical Research, Kyoto University, Uji 611-0011, Kyoto, Japan. E-mail: dkan@scl.kyoto-u.ac.jp
[d] ARC Centre of Excellence in Future Low-Energy Electronics Technologies (FLEET), UNSW Sydney, Sydney, NSW 2052, Australia
[e] Flinders Institute for Nanoscale Science and Technology, Flinders University, Adelaide, SA 5042, Australia
[f] Nanostructures Research Laboratory, Japan Fine Ceramics Center, Nagoya, Aichi 456-8587, Japan

† Electronic supplementary information (ESI) available. See DOI: https://doi.org/10.1039/d5mh00397k

‡ These authors contributed equally.

primarily attributed to the non-centrosymmetric orthorhombic phase (o-phase).[23] However, previous studies have shown that alternative mechanisms, such as uneven charge defect distribution, chemical dipole formation, strain effects, and doping, also contribute to its ferroelectricity,[25–28] and lead to some critical issues, such as the wake-up effect.[29] Furthermore, a key advantage of hafnia-based systems over conventional perovskite-structure ferroelectrics is their superior scalability. In hafnia-based thin films, the ferroelectric o-phase becomes more stable as the crystal size decreases or when interlayers are introduced to distort the lattice.[30] In contrast, polarization in classic ferroelectric films typically diminishes below a critical thickness in very thin films.[31] This highlights the crucial role of surface and interface energy in stabilizing the ferroelectric phase in hafnia-based thin films. Kelley *et al.* recently demonstrated that the surface electrochemical state can influence the ferroelectric phase transition and stability of $Hf_{0.5}Zr_{0.5}O_2$ through variations in gas environmental (pressure) and temperature.[32] Therefore, developing different strategies to modulate the electrochemical boundary conditions is essential for understanding and controlling the ferroelectricity of hafnia-based systems.

Extensive research has been conducted on interacting ferroelectric material surfaces with water molecules through mechanisms such as physical adsorption, dissociation, or chemisorption.[33,34] Among these, TiO_2-terminated perovskite oxides, including $BaTiO_3$[35,36] and $Pb(Zr_{0.2}Ti_{0.8})O_3$,[37] have been the primary focus, largely due to TiO_2-mediated surface catalysis and the ferroelectric polarization screening effect caused by ionic species dissociated from water molecules.[34] More recently, studies have also expanded to hafnia-based thin films, demonstrating that the ferroelectric imprint effect is influenced by the incorporation of moisture.[38,39] Wei *et al.* highlight the disadvantage of water adsorption, which negatively impacts domain retention and polarization stability.[39] However, the strain from the substrate,[40,41] bottom and top electrodes have a significant impact on the ferroelectric properties of HZO.[42,43] Therefore, investigating the ferroelectric properties of hafnia membranes without substrate and electrode-capping effects, particularly with respect to surface electrochemical states influenced by humidity, is essential.

In this study, we investigate the impact of humidity on the ferroelectricity of ultrathin freestanding $Hf_{0.5}Zr_{0.5}O_2$ (HZO) membranes. The HZO thin film was fabricated using pulsed laser deposition (PLD) followed by membrane exfoliation and transfer to the conductive substrate. This approach ensures the formation of the orthorhombic ferroelectric phase during the film growth process on $SrTiO_3$ (STO) substrates while preserving its ferroelectric property after exfoliation, free from the substrate-induced strain. The macroscopic ferroelectricity of HZO was confirmed in both epitaxial films and freestanding membranes through capacitance–voltage (*C–V*), polarization–electric field hysteresis (*P–E*), and current *vs.* electric field (*I–E*) measurements. Plan-view atomic-resolution observation *via* scanning transmission electron microscopy (STEM) reveals the coexistence of ferroelectric (orthorhombic) and non-ferroelectric (monoclinic) phases within the HZO membranes. Microscale polarization electrical switching behaviour and the wake-up effect are characterized using high-resolution piezo-response force microscopy (PFM) mapping and spectroscopic switching PFM (SSPFM) measurements. Additionally, humidity-dependent ferroelectricity is demonstrated using SSPFM with an integrated humidity control system in the range of 3% to 30% relative humidity (RH). A low-humidity atmosphere enhances the ferroelectricity of HZO nearly 30-fold, resulting in a ''wake-up-free'' state. This effect is attributed to modifications in the surface electrochemical state, as reduced water absorption helps maintain a high concentration of oxygen vacancies, which stabilize the ferroelectric o-phase under an applied electric field.

Results and discussion

Fig. 1(a) illustrates the preparation of a HZO freestanding membrane. Initially, the HZO thin film was epitaxially grown on a (100) $SrTiO_3$ substrate with a $La_{0.7}Sr_{0.3}MnO_3$ (LSMO) bottom electrode using PLD. Then, the sacrificing LSMO layers of the sample were selectively etched in a hydrochloric acid-based solution to exfoliate the top layer of the HZO thin film, which was subsequently transferred onto a Pt/Au-coated silicon substrate, as shown in the left panel of Fig. 1(b). Following this, top electrodes of varying diameters, ranging from 10 μm to 30 μm, were deposited for subsequent macroscopic electrical measurements, depicted as a matrix of circular electrodes in the right panel of Fig. 1(b). Both the epitaxial thin film and the freestanding membrane of HZO were characterized by X-ray diffraction measurements to confirm the crystal structure. As shown in Fig. 1(c), the main diffraction peak for the as-grown 5-nm-thick HZO appears around 29.8°, which is slightly smaller than the reported value for the orthorhombic phase (111) reflection.[44] This shift suggests the presence of in-plane compressive strain in the HZO thin film. However, after releasing the HZO film from the $SrTiO_3$ substrate, the o-(111) peak of the membrane shifts back to 30.1° in the absence of strain, as shown in Fig. 1(c) (yellow curve). This result demonstrates that the polar o-(111) phase formed during the epitaxial growth of HZO films on $SrTiO_3$ (STO) substrates is preserved even after the HZO membrane is exfoliated.

To demonstrate the macroscopic ferroelectricity of HZO and its potential application in capacitors, we performed *C–V* measurements at room temperature for both the thin film and membrane with a measurement AC frequency of 10 kHz. Fig. 1(d) presents the macroscopic *C–V* characterization of ferroelectric capacitance peaks, showing relative permittivity (ε_r) curves for as-grown and freestanding HZO. The butterfly-shaped ε_r curves, observed in the film before and after exfoliation, are characteristic of ferroelectric capacitors and can be attributed to the increased movement of domain walls near the coercive voltage (E_c).[45] The higher E_c observed in the transferred HZO membrane is attributed to the release of in-plane strain, while the presence of out-of-plane tensile strain facilitates the switching of ferroelectric polarization.[46] Additionally, we measured the room-temperature *P–E* loop for

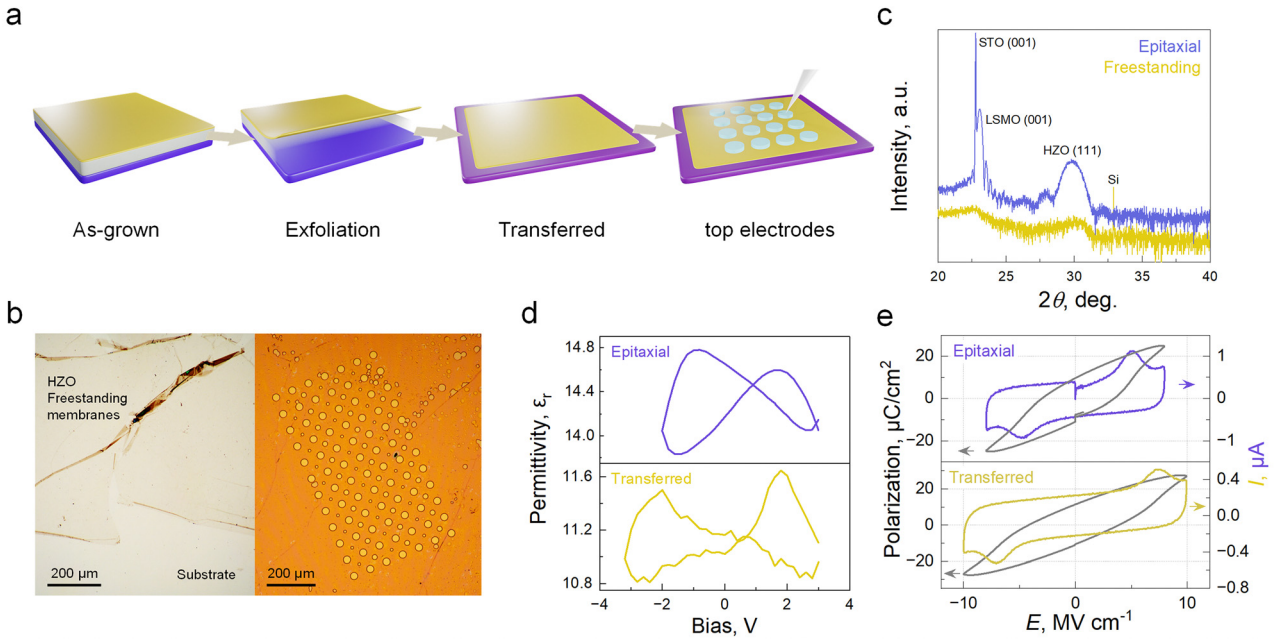

Fig. 1 Preparation of freestanding HZO films and their ferroelectricity. (a) Schematic of transferring HZO membrane followed by deposition of Au top electrodes *via* photolithography. (b) Optical microscopy of HZO freestanding membranes on substrate (left) and its Au top electrodes (right). (c) X-ray $2\theta/\theta$ diffraction patterns of the HZO epitaxial thin film on LSMO/STO substrate and its freestanding membranes on Pt/Au-coated Si substrate. (d) Macroscopic *C*–*V* characterization of ferroelectric capacitance peaks with calculated relative permittivity for HZO epitaxial film (top panel) and its membranes (bottom panel). (e) *P*–*E* hysteresis loops (red) and *I*–*E* curves (blue) of both epitaxial and transferred film.

both the transferred and as-grown thin films at 1 kHz. A distinct hysteresis loop was observed for both samples, further validating the survival of ferroelectricity in freestanding HZO membranes after the exfoliation. The *I*–*E* curves, which demonstrate the ferroelectric switching current, are shown in Fig. 1(e). The presence of two switching current peaks under positive and negative electric fields reveals the coercive voltage of the HZO films, with the transferred film exhibiting a higher value. This observation is consistent with the coercive voltage derived from *C*–*V* curves, taking into account the membrane thickness. Please note that the higher electric field required to switch the polarization in the HZO membrane can be explained by strain-influenced switching behavior in fluorite-based materials.[46] The epitaxial HZO subjected to in-plane compressive strain by the STO substrate, which induces expansion strain along the out-of-plane direction and facilitate ferroelectric switching in the out-of-plane direction.[47] Additionally, all the electrical measurements didn't involve any "wake-up" procedure.

Further electrical measurements were conducted on the HZO membrane to assess its ferroelectric performance for practical applications. A remanent polarization (P_r) of 10 μC cm^{-2} was obtained for the freestanding membranes using the positive-up-negative-down (PUND) method (Fig. S1a, ESI†). Furthermore, leakage current, polarization switching endurance, and switching time were investigated (Fig. S1b–d, ESI†), showing values comparable to those reported for ferroelectric hafnium oxide devices (ESI,† S1).

In conclusion, the present method first ensures the development of a well-oriented (111) crystalline structure of HZO thin films with an orthorhombic ferroelectric phase through the epitaxial growth of HZO on STO substrates, benefiting from favourable clamping effects during the film growth process.[48,49] Subsequently, the film is released onto different substrates to form a freestanding membrane, effectively eliminating substrate-induced strain while preserving its ferroelectric properties. It is important to note that direct deposition of HZO on conductive substrates without exfoliation may induce undesirable strain due to mismatches in lattice parameters and thermal expansion coefficients between HZO and the substrate.[50–55]

For the identification of the crystal structure of HZO, we conduct plan-view high-angle annular dark-field (HAADF) STEM characterization, which visualizes cation arrangements directly, by transferring the freestanding HZO membrane onto a holey carbon film supported by a Cu grid. Fig. 2(a) shows the HAADF STEM image, visualizing HZO with three different types of crystallographic phase and grain sizes ranging from 5 to 20 nm. Each type of phase can be identified as (111)-oriented orthorhombic (o) phase in Fig. 2(b), (001)-oriented orthorhombic phase in Fig. 2(c) and (−111)-oriented monoclinic (m) phase in Fig. 2(d) with their fast Fourier transform (FFT) patterns and structural models on the side (hafnium/zirconium atom in blue and oxygen atom in red). The presence of m-phase and o-phase provided the possibility of phase transformation, which could be the origin of "wake up" and "fatigue" behaviour.[56] To conclude, we identified that the dominant phase of HZO film is the ferroelectric orthorhombic phase and its polymorphic nature.

The freestanding HZO membrane, with a thickness below 5 nm and free from substrate-induced strain, allows its ferroelectric properties to be closely coupled with the surface

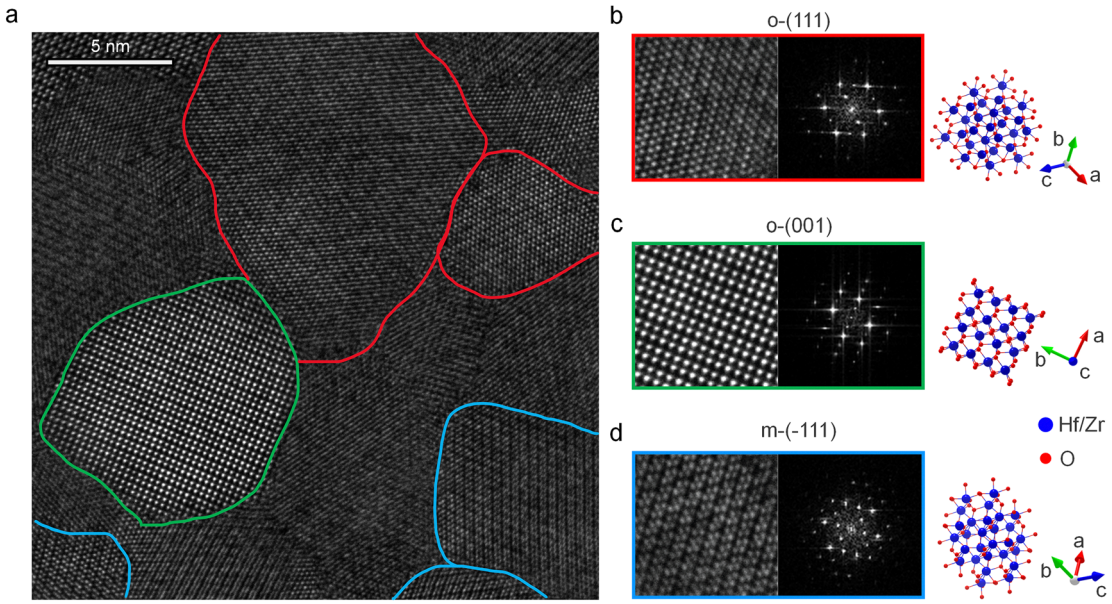

Fig. 2 Identification of crystallographic phases of HZO membrane. (a) Plan-view HAADF-STEM image. Orthorhombic phases oriented along the (b) (111), (c) (001) direction, and (d) monoclinic phases oriented along the (−111) direction with corresponding FFT patterns and crystal structures on the right.

electrochemical state. In this study, we microscopically examined the ferroelectricity of HZO freestanding membranes and explored the influence of environmental conditions. To achieve this, we performed a series of PFM measurements under both ambient (∼50% RH) and ultra-low humidity conditions (3% RH), as shown in Fig. 3. A well-defined domain wall and 180° phase contrast were observed after box-in-box poling with a −8 V (0.8 μm × 0.8 μm) and +8 V (1.5 μm × 1.5 μm) dc bias, demonstrating the polarization's electrical switchability under 3% RH (Fig. 3(a) and (b)). Notably, the contrast between the unpoled and −8 V poled areas is similar, indicating a pristine upward-oriented polarization of the HZO. The atomic force microscopy has also been conducted in a 2 μm area, showing a smooth surface with an RMS roughness of 400 pm (Fig. S2a, ESI†). Additionally, local bias-dependent spectroscopic switching PFM (SSPFM) measurements further confirm that the ferroelectric properties of the HZO film remain well-preserved after exfoliation under low humidity conditions. This is evidenced by the robust butterfly-shaped amplitude loop and 180° phase hysteresis loop shown in Fig. 3(c) and Fig. S3 (ESI†) for

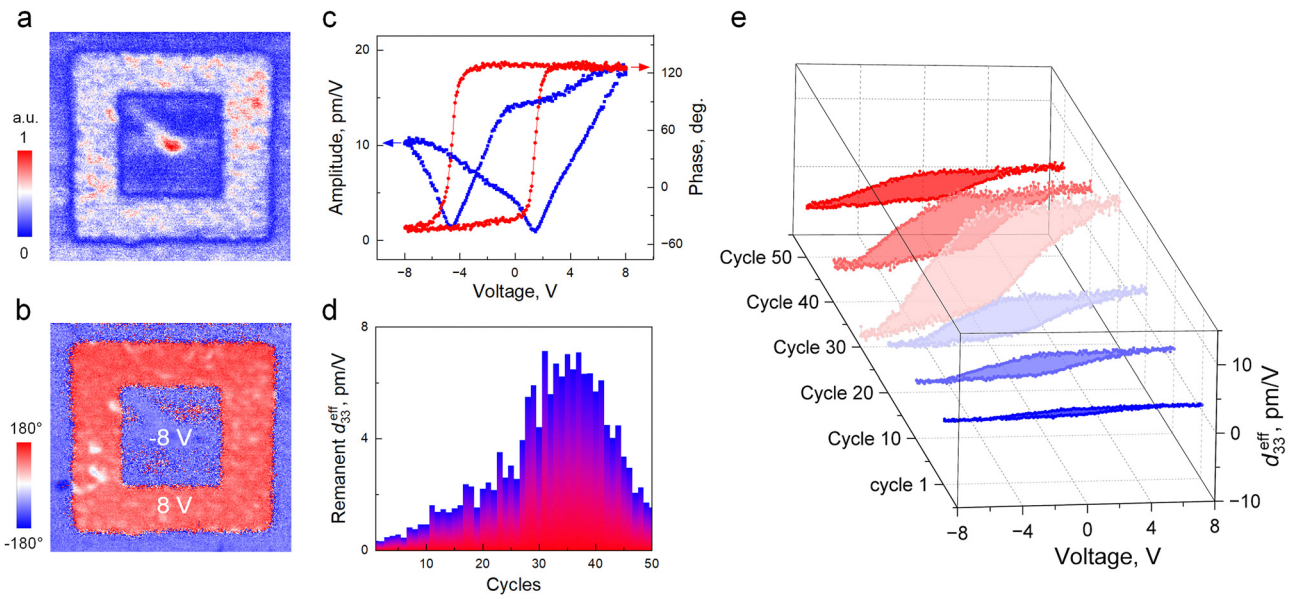

Fig. 3 Electric polarization switching in freestanding HZO membranes and wakeup phenomenon. Out-of-plane PFM (a) amplitude and (b) phase images after ±8 V box-in-box poling. (c) PFM butterfly loop for amplitude (blue) and hysteresis loop (red) for phase. (d) Remanent d_{33}^{eff} as a function of the cycles number. (e) PFM hysteresis loops for cycles no. 1, 10, 20, 30, 40 and 50.

50 cycles, without the need for a "wake-up" process, consistent with the results from macroscopic measurements. The surface conditions in this case are analogous to those in macroscopic measurements, where the surface is covered by an electrode and free from water molecules in the surrounding air. In contrast, under ambient conditions (RH 60%), the same area cannot be poled, indicating weak polarization switching behaviour (Fig. S2b and c, ESI†). Additionally, a wake-up process was observed through SSPFM measurements, where the development of ferroelectricity was found to depend on the number of cycles. This result is consistent with previous studies showing that high-humidity environments commonly induce a wake-up effect.[38] As shown in Fig. 3(e), the remanent d_{33}^{eff} value from the hysteresis loops increased approximately 20-fold, reaching a peak around cycle no. 35, followed by a subsequent decline. This behaviour is consistent with previous findings, where cycle no. 1–35 corresponds to the wake-up effect driven by a field-cycling-induced phase transition from the non-ferroelectric monoclinic phase to the ferroelectric orthorhombic phase.[3,57,58] Cycles no. 35–50, however, mark the onset of fatigue, attributed to the increase in defect density.[58] It is important to note that the accelerated wake-up and fatigue effects can be attributed to the microstructural field cycling applied through the tip to the freestanding membrane, which lacks the clamping strain from the substrate that would otherwise constrain the phase transformation.

Next, to gain deeper insight into the impact of humidity on the ferroelectric properties of HZO, we varied the atmospheric humidity during measurements. Fig. 4(a) demonstrates that as the humidity level increases from 3% to 30%, the amplitude of the hysteresis loop gradually decreases. The remanent d_{33}^{eff} values, extracted from the PFM hysteresis loops at each humidity level, are plotted in Fig. 4(b). Initially, the piezoresponse decreases linearly with increasing humidity, from ~9 pm V^{-1} at 3% RH to ~2 pm V^{-1} at 8% RH, before gradually declining further to 0.3 pm V^{-1} at 30% RH. This indicates that an ultra-low humidity environment enhances the ferroelectricity by nearly 30-fold. To exclude the influence of extrinsic effects such as ionic motion, electrostatic forces, or Vegard strains in the humidity-driven changes, we conducted the first and second harmonic frequency response measurements of HZO using a small AC across a broad frequency range. The results in Fig. 4(c) indicate that ferroelectricity remains the dominant intrinsic effect under both 3% and 30% RH conditions. At ultra-low humidity levels (3% RH), the amplitude of the first harmonic response shows a marked increase, aligning with the higher d_{33}^{eff} values presented in Fig. 4(a). This behaviour can be attributed to the effect of humidity on the electrochemical state of the HZO surface. Kelley *et al.* found that in a pristine upward-polarization HZO thin film (similar to ours), a low-oxygen-pressure environment—akin to low humidity conditions—reduces compensatory mechanisms by limiting the adsorption of surface adsorbates or ionic species from the atmosphere. This reduction in surface oxygen content increases the negative surface charge, thereby enhancing the ferroelectric stability of HZO.[32] Moreover, previous studies[38] indicate that polarization is more sensitive to humidity levels than to oxygen conditions, as the incorporation of hydroxide ions from humid atmospheres is more efficient than that of oxygen. This suggests that low-humidity environments may offer comparable or even more superior ferroelectric stability for HZO relative to Kelley's findings regarding oxygen.

In addition, oxygen vacancies, as a predominant intrinsic defect in HfO_2-based thin films, are unavoidable and commonly present at relatively high concentrations, around 1.7×10^{21} cm^{-3}.[28,59] Surface oxygen vacancies are known to promote water dissociation with water acting as an oxidizing agent that fills and deactivates these vacancies.[60,61] Specifically, an OH^- occupies one oxygen vacancy ($V_O^{\bullet\bullet}$), while a proton bonds to a neighbouring oxygen site (O_O), resulting in a pair of positively charged $OH^\bullet$ ions ($OH_O^\bullet$) within the lattice, as illustrated in the following equation:[38,62,63]

$$H_2O(g) + V_O^{\bullet\bullet} + O_O \rightarrow 2OH_O^\bullet \quad (1)$$

Thus, low-humidity conditions maintain a higher concentration of active oxygen vacancies. These vacancies have been shown to stabilize or promote the polar orthorhombic phase

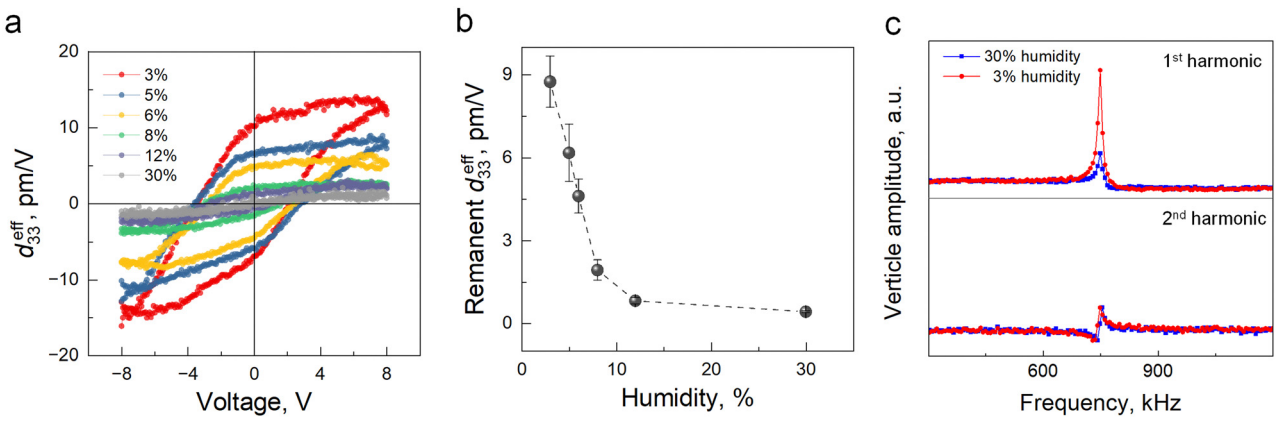

Fig. 4 Humidity-dependent ferroelectric behaviour. (a) PFM hysteresis loops at 3% to 30% RH atmosphere and their (b) remanent d_{33}^{eff} as a function of humidity. (c) The first and second harmonic response for HZO membranes at 3% and 30% RH atmosphere.

transition under an electric field while suppressing the formation of the monoclinic (m) phase, thereby enhancing the ferroelectric properties of HfO_2-based materials.[64–68]

In a low-humidity environment (RH 2.5–10%), hydroxyl (OH) groups strongly chemisorb onto the surface of metal oxides, forming a discontinuous sub-monolayer of water.[33,34,69] Given the limited availability of water molecules within this low RH range, water absorption by the material positively correlates with humidity levels, resulting in the gradual occupation of oxygen vacancies as humidity increases, which ultimately reduces the ferroelectricity of HZO.[70,71] However, when humidity exceeds 10% RH, additional water layers have limited influence on the sample surface once the first monolayer is complete. This phenomenon may give rise to the two-phase behaviour of HZO d_{33}^{eff} as a function of RH, with distinct regimes observed between 3–8% RH and 8–30% RH, as shown in Fig. 4(b).

Conclusion

In summary, we have identified a humidity-dependent ferroelectric behaviour in 5 nm ultrathin freestanding HZO membranes, free from substrate and electrode-capping effects. These membranes were fabricated using pulsed laser deposition (PLD) on an STO substrate to form the polar o-(111) phase, then exfoliated and transferred onto a Si substrate while retaining their ferroelectric properties. Macroscopic ferroelectricity in the membranes was confirmed through electrical measurements (*P–E*, *I–E*, and *C–V*), highlighting the potential of HZO for capacitor applications. Crystallographic analysis using plan-view atomic-resolution STEM observation revealed the coexistence of orthorhombic and monoclinic phases, which supports the wake-up behaviour arising from phase transitions. Further investigation of nanoscale polarization switching through PFM techniques and spectroscopic piezoresponse measurements on a free surface demonstrated a negative correlation between ferroelectricity and relative humidity (RH). This behaviour is attributed to the effect of humidity on the electrochemical conditions of the HZO surface. By reducing surface water adsorption, a higher concentration of oxygen vacancies can be maintained, promoting the stability of the ferroelectric phase under an electric field.

Overall, this study presents a novel approach to tuning surface electrochemical conditions while mitigating the wake-up effect in HZO. We demonstrate the coexistence of two key mechanisms—field-cycling-induced phase transitions and humidity-modulated surface electrochemical state that can be leveraged to optimize the ferroelectric properties of HZO membranes. These findings offer valuable insights for the development and optimization of other binary oxide-based devices.

Methods

Sample preparation

The freestanding hafnia membranes were prepared by selective etching of the LSMO buffer layer in STO/LSMO/HZO epitaxial heterostructures, which were prepared by pulsed laser deposition (PLD). The detailed deposition conditions were reported previously.[72] The etchant contains 5 wt% hydrochloric acid and 0.05 M potassium iodide, which is known to effectively etch the Mn-based perovskite layer.[73] The Si substrate was coated with sputter-deposited Pt/Au layers for better conductivity prior to the conventional dry transfer method. The whole transfer process of freestanding membranes to conductive substrates is detailed in our previous work.[74]

Structural characterization

XRD $2\theta/\theta$ diffraction patterns were measured with a four-circle diffractometer (X'Pert MRD, PANalytical) using Cu Kα1 radiation. The HAADF STEM image was obtained using a JEOL JEM-ARM300F2 equipped with aberration correctors. The accelerating voltage and probe forming half-angle were set to be 300 keV and 24 mrad, respectively.

Electrical measurement

The electrical measurements were performed on metal–insulator–metal (MIM) structures by depositing gold pads ($\varnothing$ 10–30 μm) on top of HZO through photolithography and thermal evaporation. The LSMO and p-type silicon layers served as bottom electrodes for epitaxial and freestanding HZO samples, respectively. Polarization hysteresis loops and PUND (positive-up-negative-down) measurements were conducted by using ferroelectric testers (TOYO Tech, FCE-10) with a measurement frequency of 1 kHz at room temperature. The capacitance butterfly curves were measured by the LCR meter and later converted to the dielectric constant.

Scanning probe microscopy

Scanning probe microscopy measurements were conducted using an AIST-NT Smart SPM 1000 under ambient conditions with a built-in humidity controller. Conductive platinum-coated tips (Mikromasch HQ: NSC35/Pt) with a force constant of $\sim$5.4 N m^{-1} were employed for the measurements. During PFM measurements, a modulating voltage of 1 V (peak-to-peak) at a frequency of 750 kHz was applied. Spectroscopic PFM hysteresis loops were recorded by introducing a triangular DC bias waveform along with small-signal AC modulation. For all SSPFM measurements, the tip has been calibrated using the thermal noise method.[75] Throughout all SPM experiments, the bias was applied to the conductive nanoscale tip, with the sample grounded on a conductive metal plate to complete the electrical circuit.

Data availability

The data supporting this article have been included as part of the ESI.†

Conflicts of interest

The authors declare no conflict of interest.

Acknowledgements

We acknowledge the financial support provided by the UNSW-MAHE collaboration seed grant (RG194284-D). We further acknowledge support from ARC discovery grants and the ARC Centre of Excellence in Future Low-Energy Technologies (FLEET). This work was partly supported by Grants-in-Aid for Scientific Research (no. 23KJ1239, 23H05457, and 24H01190) and by grants for the Integrated Research Consortium on Chemical Sciences and the International Collaborative Research Program of the Institute for Chemical Research in Kyoto University from the Ministry of Education, Culture, Sports, Science, and Technology (MEXT) of Japan. The work was also supported by the Japan Science and Technology Agency (JST) as part of PRESTO, Grant No. JPMJPR24H3, and the Adopting Sustainable Partnerships for Innovative Research Ecosystem (ASPIRE), grant no. JPMJAP2312 and JPMJAP2314. STEM images were acquired using a transmission electron microscope installed through the Innovative Science and Technology Initiative for Security, Grant Number JPJ004596, from the Acquisition, Technology, and Logistics Agency (ATLA), Japan. The work was also supported by The Samco Foundation.

References

1 T. Böscke, S. Teichert, D. Bräuhaus, J. Müller, U. Schröder, U. Böttger and T. Mikolajick, Phase transitions in ferroelectric silicon doped hafnium oxide, *Appl. Phys. Lett.*, 2011, **99**(11), 112904.

2 J. Müller, T. Böscke, D. Bräuhaus, U. Schröder, U. Böttger, J. Sundqvist, P. Kücher, T. Mikolajick and L. Frey, Ferroelectric $Zr_{0.5}Hf_{0.5}O_2$ thin films for nonvolatile memory applications, *Appl. Phys. Lett.*, 2011, **99**(11), 112901.

3 J. Müller, E. Yurchuk, T. Schlösser, J. Paul, R. Hoffmann, S. Müller, D. Martin, S. Slesazeck, P. Polakowski and J. Sundqvist, Ferroelectricity in HfO_2 enables nonvolatile data storage in 28 nm HKMG, In 2012 symp. on VLSI tech. (VLSIT), 2012, IEEE, pp. 25–26.

4 T. Mikolajick, S. Slesazeck, M. H. Park and U. Schroeder, Ferroelectric hafnium oxide for ferroelectric random-access memories and ferroelectric field-effect transistors, *MRS Bull.*, 2018, **43**(5), 340–346.

5 M. H. Park, H. J. Kim, Y. J. Kim, T. Moon, K. Do Kim and C. S. Hwang, Toward a multifunctional monolithic device based on pyroelectricity and the electrocaloric effect of thin antiferroelectric $Hf_xZr_{1-x}O_2$ films, *Nano Energy*, 2015, **12**, 131–140.

6 M. Hoffmann, U. Schroeder, C. Künneth, A. Kersch, S. Starschich, U. Böttger and T. Mikolajick, Ferroelectric phase transitions in nanoscale HfO_2 films enable giant pyroelectric energy conversion and highly efficient supercapacitors, *Nano Energy*, 2015, **18**, 154–164.

7 M. H. Park, H. J. Kim, Y. J. Kim, T. Moon, K. D. Kim and C. S. Hwang, Thin Hf_xZr_{1-x} O_2 Films: A New Lead-Free System for Electrostatic Supercapacitors with Large Energy Storage Density and Robust Thermal Stability, *Adv. Energy Mater.*, 2014, **4**(16), 1400610.

8 K. Do Kim, Y. H. Lee, T. Gwon, Y. J. Kim, H. J. Kim, T. Moon, S. D. Hyun, H. W. Park, M. H. Park and C. S. Hwang, Scale-up and optimization of HfO_2–ZrO_2 solid solution thin films for the electrostatic supercapacitors, *Nano Energy*, 2017, **39**, 390–399.

9 K. Ni, P. Sharma, J. Zhang, M. Jerry, J. A. Smith, K. Tapily, R. Clark, S. Mahapatra and S. Datta, Critical role of interlayer in $Hf_{0.5}$ $Zr_{0.5}O_2$ ferroelectric FET nonvolatile memory performance, *IEEE Trans. Electron Devices*, 2018, **65**(6), 2461–2469.

10 H. Mulaosmanovic, J. Ocker, S. Müller, U. Schroeder, J. Müller, P. Polakowski, S. Flachowsky, R. van Bentum, T. Mikolajick and S. Slesazeck, Switching kinetics in nanoscale hafnium oxide based ferroelectric field-effect transistors, *ACS Appl. Mater. Interfaces*, 2017, **9**(4), 3792–3798.

11 K. Chatterjee, S. Kim, G. Karbasian, A. J. Tan, A. K. Yadav, A. I. Khan, C. Hu and S. Salahuddin, Self-aligned, gate last, FDSOI, ferroelectric gate memory device with 5.5-nm $Hf_{0.8}$ $Zr_{0.2}O_2$, high endurance and breakdown recovery, *IEEE Electron Device Lett.*, 2017, **38**(10), 1379–1382.

12 A. G. Chernikova, M. G. Kozodaev, D. V. Negrov, E. V. Korostylev, M. H. Park, U. Schroeder, C. S. Hwang and A. M. Markeev, Improved ferroelectric switching endurance of La-doped $Hf_{0.5}Zr_{0.5}O_2$ thin films, *ACS Appl. Mater. Interfaces*, 2018, **10**(3), 2701–2708.

13 F. Mo, Y. Tagawa, T. Saraya, T. Hiramoto and M. Kobayashi, Scalability study on fcrroclcctric-HfO_2 tunnel junction memory based on non-equilibrium green function method with self-consistent potential, In 2018 IEEE Int. Electron Devices Mtg. (IEDM), 2018, IEEE, pp. 16.13. 11–16.13. 14.

14 B. Max, M. Hoffmann, S. Slesazeck and T. Mikolajick, Ferroelectric tunnel junctions based on ferroelectric-dielectric $Hf_{0.5}Zr_{0.5}O_2/Al_2O_3$ capacitor stacks. In 2018 48th Eu. Solid-State Device Res. Conf. (ESSDERC), 2018, IEEE, pp. 142–145.

15 M. Kobayashi, Y. Tagawa, F. Mo, T. Saraya and T. Hiramoto, Ferroelectric HfO_2 tunnel junction memory with high TER and multi-level operation featuring metal replacement process, *IEEE J. Electron Devices Soc.*, 2018, **7**, 134–139.

16 S. S. Cheema, N. Shanker, C. H. Hsu, A. Datar, J. Bae, D. Kwon and S. Salahuddin, One nanometer HfO_2-based ferroelectric tunnel junctions on silicon, *Adv. Electron. Mater.*, 2022, **8**(6), 2100499.

17 S. Fichtner, N. Wolff, F. Lofink, L. Kienle and B. Wagner, AlScN: A III-V semiconductor based ferroelectric, *J. Appl. Phys.*, 2019, **125**(11), 114103.

18 K. Ferri, S. Bachu, W. Zhu, M. Imperatore, J. Hayden, N. Alem, N. Giebink, S. Trolier-McKinstry and J.-P. Maria, Ferroelectrics everywhere: Ferroelectricity in magnesium substituted zinc oxide thin films, *J. Appl. Phys.*, 2021, **130**(4), 044101.

19 H. Zhang, A. Alanthattil, R. F. Webster, D. Zhang, M. B. Ghasemian, R. B. Venkataramana, J. Seidel and P. Sharma, Robust switchable polarization and coupled electronic characteristics of magnesium-doped zinc oxide, *ACS Nano*, 2023, **17**(17), 17148–17157.

20 H. Zhang, A. Ayana, R. F. Webster, M. B. Ghasemian, B. V. Rajendra, J. Seidel and P. Sharma, Polarity Control of the Schottky Barrier in Wurtzite Ferroelectrics, *ACS Appl. Electron. Mater.*, 2024, **6**(3), 1951–1958.

21 A. Ayana, H. Zhang, D. Chu, J. Seidel, B. Rajendra and P. Sharma, Impact of aliovalent La-doping on zinc oxide–A wurtzite piezoelectric, *Mater. Sci. Semicond. Process.*, 2024, **181**, 108617.
22 T. D. Huan, V. Sharma, G. A. Rossetti Jr and R. Ramprasad, Pathways towards ferroelectricity in hafnia, *Phys. Rev. B: Condens. Matter Mater. Phys.*, 2014, **90**(6), 064111.
23 R. Materlik, C. Künneth and A. Kersch, The origin of ferroelectricity in $Hf_{1-x}Zr_xO_2$: A computational investigation and a surface energy model, *J. Appl. Phys.*, 2015, **117**(13), 134109.
24 Y. Wei, P. Nukala, M. Salverda, S. Matzen, H. J. Zhao, J. Momand, A. S. Everhardt, G. Agnus, G. R. Blake and P. Lecoeur, A rhombohedral ferroelectric phase in epitaxially strained $Hf_{0.5}Zr_{0.5}O_2$ thin films, *Nat. Mater.*, 2018, **17**(12), 1095–1100.
25 R. Batra, T. D. Huan, J. L. Jones, G. Rossetti Jr and R. Ramprasad, Factors favoring ferroelectricity in hafnia: A first-principles computational study, *J. Phys. Chem. C*, 2017, **121**(8), 4139–4145.
26 D. Martin, J. Müller, T. Schenk, T. M. Arruda, A. Kumar, E. Strelcov, E. Yurchuk, S. Müller, D. Pohl and U. Schröder, Ferroelectricity in Si-doped HfO_2 revealed: a binary lead-free ferroelectric, *Adv. Mater.*, 2014, **26**(48), 8198–8202.
27 S. Zhou, J. Zhang and A. M. Rappe, Strain-induced antipolar phase in hafnia stabilizes robust thin-film ferroelectricity, *Sci. Adv.*, 2022, **8**(47), eadd5953.
28 M. Pešić, F. P. G. Fengler, L. Larcher, A. Padovani, T. Schenk, E. D. Grimley, X. Sang, J. M. LeBeau, S. Slesazeck and U. Schroeder, Physical mechanisms behind the field-cycling behavior of HfO_2-based ferroelectric capacitors, *Adv. Funct. Mater.*, 2016, **26**(25), 4601–4612.
29 M. H. Park, Y. H. Lee, T. Mikolajick, U. Schroeder and C. S. Hwang, Review and perspective on ferroelectric HfO_2-based thin films for memory applications, *MRS Commun.*, 2018, **8**(3), 795–808.
30 J. F. Ihlefeld, S. T. Jaszewski and S. S. Fields, A Perspective on ferroelectricity in hafnium oxide: Mechanisms and considerations regarding its stability and performance, *Appl. Phys. Lett.*, 2022, **121**(24), 240502.
31 J. F. Ihlefeld, D. T. Harris, R. Keech, J. L. Jones, J. P. Maria and S. Trolier-McKinstry, Scaling effects in perovskite ferroelectrics: fundamental limits and process–structure–property relations, *J. Am. Ceram. Soc.*, 2016, **99**(8), 2537–2557.
32 K. P. Kelley, A. N. Morozovska, E. A. Eliseev, Y. Liu, S. S. Fields, S. T. Jaszewski, T. Mimura, S. Calderon, E. C. Dickey and J. F. Ihlefeld, Ferroelectricity in hafnia controlled via surface electrochemical state, *Nat. Mater.*, 2023, **22**(9), 1144–1151.
33 N. Domingo, E. Pach, K. Cordero-Edwards, V. Pérez-Dieste, C. Escudero and A. Verdaguer, Water adsorption, dissociation and oxidation on $SrTiO_3$ and ferroelectric surfaces revealed by ambient pressure X-ray photoelectron spectroscopy, *Phys. Chem. Chem. Phys.*, 2019, **21**(9), 4920–4930.
34 I. Spasojevic, A. Verdaguer, G. Catalan and N. Domingo, Effect of humidity on the writing speed and domain wall dynamics of ferroelectric domains, *Adv. Electron. Mater.*, 2022, **8**(6), 2100650.
35 X. Li, B. Wang, T.-Y. Zhang and Y. Su, Water adsorption and dissociation on $BaTiO_3$ single-crystal surfaces, *J. Phys. Chem. C*, 2014, **118**(29), 15910–15918.
36 J. Wang, F. Gaillard, A. Pancotti, B. Gautier, G. Niu, B. Vilquin, V. Pillard, G. Rodrigues and N. Barrett, Chemistry and atomic distortion at the surface of an epitaxial $BaTiO_3$ thin film after dissociative adsorption of water, *J. Phys. Chem. C*, 2012, **116**(41), 21802–21809.
37 J. J. Segura, N. Domingo, J. Fraxedas and A. Verdaguer, Surface screening of written ferroelectric domains in ambient conditions, *J. Appl. Phys.*, 2013, **113**(18), 187213.
38 F. Berg, N. Kopperberg, J. Lübben, I. Valov, X. Wu, U. Simon and U. Böttger, Influence of moisture on the ferroelectric properties of sputtered hafnium oxide thin films, *J. Appl. Phys.*, 2023, **134**(18), 185106.
39 L. Q. Wei, Z. Guan, W. Y. Tong, W. C. Fan, A. Mattursun, B. B. Chen, P. H. Xiang, G. Han, C. G. Duan and N. Zhong, Ambient Moisture-Induced Self Alignment of Polarization in Ferroelectric Hafnia, *Adv. Sci.*, 2024, 2410354.
40 T. Shiraishi, K. Katayama, T. Yokouchi, T. Shimizu, T. Oikawa, O. Sakata, H. Uchida, Y. Imai, T. Kiguchi and T. J. Konno, Impact of mechanical stress on ferroelectricity in $(Hf_{0.5}Zr_{0.5})O_2$ thin films, *Appl. Phys. Lett.*, 2016, **108**(26), 262904.
41 S. Liu and B. M. Hanrahan, Effects of growth orientations and epitaxial strains on phase stability of HfO_2 thin films, *Phys. Rev. Mater.*, 2019, **3**(5), 054404.
42 Y. Goh and S. Jeon, The effect of the bottom electrode on ferroelectric tunnel junctions based on CMOS-compatible HfO_2, *Nanotechnology*, 2018, **29**(33), 335201.
43 R. Cao, Y. Wang, S. Zhao, Y. Yang, X. Zhao, W. Wang, X. Zhang, H. Lv, Q. Liu and M. Liu, Effects of capping electrode on ferroelectric properties of $Hf_{0.5}Zr_{0.5}O_2$ thin films, *IEEE Electron Device Lett.*, 2018, **39**(8), 1207–1210.
44 M. Hyuk Park, H. Joon Kim, Y. Jin Kim, W. Lee, T. Moon and C. Seong Hwang, Evolution of phases and ferroelectric properties of thin $Hf_{0.5}Zr_{0.5}O_2$ films according to the thickness and annealing temperature, *Appl. Phys. Lett.*, 2013, **102**(24), 242905.
45 D. Bolten, O. Lohse, M. Grossmann and R. Waser, Reversible and irreversible domain wall contributions to the polarization in ferroelectric thin films, *Ferroelectrics*, 1999, **221**(1), 251–257.
46 B. Xu, P. D. Lomenzo, A. Kersch, T. Schenk, C. Richter, C. M. Fancher, S. Starschich, F. Berg, P. Reinig and K. M. Holsgrove, Strain as a global factor in stabilizing the ferroelectric properties of ZrO_2, *Adv. Funct. Mater.*, 2024, **34**(8), 2311825.
47 Y. Wei, P. Nukala, M. Salverda, S. Matzen, H. J. Zhao, J. Momand, A. S. Everhardt, G. Agnus, G. R. Blake and P. Lecoeur, A rhombohedral ferroelectric phase in epitaxially strained $Hf_{0.5}Zr_{0.5}O_2$ thin films, *Nat. Mater.*, 2018, **17**(12), 1095–1100.
48 Y. Shen, K. Ooe, X. Yuan, T. Yamada, S. Kobayashi, M. Haruta, D. Kan and Y. Shimakawa, Ferroelectric free-standing hafnia membranes with metastable rhombohedral structure down to 1-nm-thick, *Nat. Commun.*, 2024, **15**(1), 4789, DOI: **10.1038/s41467-024-49055-w** From NLM PubMed-not-MEDLINE.
49 H. Zhong, M. Li, Q. Zhang, L. Yang, R. He, F. Liu, Z. Liu, G. Li, Q. Sun and D. Xie, Large-Scale $Hf_{0.5}Zr_{0.5}O_2$

Membranes with Robust Ferroelectricity, *Adv. Mater.*, 2022, **34**(24), 2109889.

50 I. Fina and F. Sanchez, Epitaxial ferroelectric HfO_2 films: growth, properties, and devices, *ACS Appl. Electron. Mater.*, 2021, **3**(4), 1530–1549.

51 Y.-W. Chen and C. Liu, Effects of shear strain on HZO ferroelectric orthorhombic phases, *Appl. Phys. Lett.*, 2023, **123**(11), 112901.

52 R. Patil and E. Subbarao, Axial thermal expansion of ZrO_2 and HfO_2 in the range room temperature to 1400 °C, *J. Appl. Crystallogr.*, 1969, **2**(6), 281–288.

53 Y. Kim, M. Watanabe, J. Matsuda, J. T. Song, A. Takagaki, A. Staykov and T. Ishihara, Tensile strain for band engineering of $SrTiO_3$ for increasing photocatalytic activity to water splitting, *Appl. Catal., B*, 2020, **278**, 119292.

54 G. White and J. Collins, Thermal expansion of copper, silver, and gold at low temperatures, *J. Low Temp. Phys.*, 1972, **7**, 43–75.

55 A. Rahman, A. Rahman, W. Ghann, H. Kang and J. Uddin, Terahertz multispectral imaging for the analysis of gold nanoparticles' size and the number of unit cells in comparison with other techniques, *Int. J. biosens. bioelectron*, 2018, **4**, 159–164.

56 S. S. Fields, S. W. Smith, P. J. Ryan, S. T. Jaszewski, I. A. Brummel, A. Salanova, G. Esteves, S. L. Wolfley, M. D. Henry and P. S. Davids, Phase-exchange-driven wake-up and fatigue in ferroelectric hafnium zirconium oxide films, *ACS Appl. Mater. Interfaces*, 2020, **12**(23), 26577–26585.

57 P. D. Lomenzo, Q. Takmeel, C. Zhou, C. M. Fancher, E. Lambers, N. G. Rudawski, J. L. Jones, S. Moghaddam and T. Nishida, TaN interface properties and electric field cycling effects on ferroelectric Si-doped HfO_2 thin films, *J. Appl. Phys.*, 2015, **117**(13), 134105.

58 E. D. Grimley, T. Schenk, X. Sang, M. Pešić, U. Schroeder, T. Mikolajick and J. M. LeBeau, Structural changes underlying field-cycling phenomena in ferroelectric HfO_2 thin films, *Adv. Electron. Mater.*, 2016, **2**(9), 1600173.

59 S. Zafar, H. Jagannathan, L. F. Edge and D. Gupta, Measurement of oxygen diffusion in nanometer scale HfO_2 gate dielectric films, *Appl. Phys. Lett.*, 2011, **98**(15), 152903.

60 W. Li, S. Liu, S. Wang, Q. Guo and J. Guo, The roles of reduced Ti cations and oxygen vacancies in water adsorption and dissociation on $SrTiO_3$ (110), *J. Phys. Chem. C*, 2014, **118**(5), 2469–2474.

61 H. Li, P. Zhang, J. Jia, X. Wang and S. Rong, A cobalt-vacant Co_3O_4 as a stable catalyst for room-temperature decomposition of ozone in humid air, *Appl. Catal., B*, 2024, **340**, 123222.

62 G. Ketteler, S. Yamamoto, H. Bluhm, K. Andersson, D. E. Starr, D. F. Ogletree, H. Ogasawara, A. Nilsson and M. Salmeron, The nature of water nucleation sites on TiO2 (110) surfaces revealed by ambient pressure X-ray photoelectron spectroscopy, *J. Phys. Chem. C*, 2007, **111**(23), 8278–8282.

63 N. Domingo, E. Pach, K. Cordero-Edwards, V. Pérez-Dieste, C. Escudero and A. Verdaguer, Water adsorption, dissociation and oxidation on $SrTiO_3$ and ferroelectric surfaces revealed by ambient pressure X-ray photoelectron spectroscopy, *Phys. Chem. Chem. Phys.*, 2019, **21**(9), 4920–4930.

64 Y. H. Lee, H. J. Kim, T. Moon, K. Do Kim, S. D. Hyun, H. W. Park, Y. B. Lee, M. H. Park and C. S. Hwang, Preparation and characterization of ferroelectric $Hf_{0.5}Zr_{0.5}O_2$ thin films grown by reactive sputtering, *Nanotechnology*, 2017, **28**(30), 305703.

65 U. Schroeder, M. H. Park, T. Mikolajick and C. S. Hwang, The fundamentals and applications of ferroelectric HfO_2, *Nat. Rev. Mater.*, 2022, **7**(8), 653–669.

66 M. D. Glinchuk, A. N. Morozovska, A. Lukowiak, W. Stręk, M. V. Silibin, D. V. Karpinsky, Y. Kim and S. V. Kalinin, Possible electrochemical origin of ferroelectricity in HfO_2 thin films, *J. Alloys Compd.*, 2020, **830**, 153628.

67 M. Hoffmann, U. Schroeder, T. Schenk, T. Shimizu, H. Funakubo, O. Sakata, D. Pohl, M. Drescher, C. Adelmann and R. Materlik, Stabilizing the ferroelectric phase in doped hafnium oxide, *J. Appl. Phys.*, 2015, **118**(7), 072006.

68 Y. Zhou, Y. Zhang, Q. Yang, J. Jiang, P. Fan, M. Liao and Y. Zhou, The effects of oxygen vacancies on ferroelectric phase transition of HfO_2-based thin film from first-principle, *Comput. Mater. Sci.*, 2019, **167**, 143–150.

69 N. Domingo, I. Gaponenko, K. Cordero-Edwards, N. Stucki, V. Pérez-Dieste, C. Escudero, E. Pach, A. Verdaguer and P. Paruch, Surface charged species and electrochemistry of ferroelectric thin films, *Nanoscale*, 2019, **11**(38), 17920–17930.

70 A. Verdaguer, J. J. Segura, J. Fraxedas, H. Bluhm and M. Salmeron, Correlation between charge state of insulating NaCl surfaces and ionic mobility induced by water adsorption: a combined ambient pressure X-ray photoelectron spectroscopy and scanning force microscopy study, *J. Phys. Chem. C*, 2008, **112**(43), 16898–16901.

71 K. Cordero-Edwards, L. Rodríguez, A. Calo, M. J. Esplandiu, V. Pérez-Dieste, C. Escudero, N. Domingo and A. Verdaguer, Water affinity and surface charging at the z-cut and y-cut $LiNbO_3$ surfaces: an ambient pressure X-ray photoelectron spectroscopy study, *J. Phys. Chem. C*, 2016, **120**(42), 24048–24055.

72 Y. Shen, M. Haruta, I.-C. Lin, L. Xie, D. Kan and Y. Shimakawa, Stabilization of ferroelectric $Hf_{0.5}Zr_{0.5}O_2$ epitaxial films *via* monolayer reconstruction driven by valence-dependent interfacial redox reaction and intralayer electron transfer, *Phys. Rev. Mater.*, 2023, **7**(11), 114405.

73 D. Pesquera, E. Parsonnet, A. Qualls, R. Xu, A. J. Gubser, J. Kim, Y. Jiang, G. Velarde, Y. L. Huang and H. Y. Hwang, Beyond substrates: strain engineering of ferroelectric membranes, *Adv. Mater.*, 2020, **32**(43), 2003780.

74 Y. Shen, K. Ooe, X. Yuan, T. Yamada, S. Kobayashi, M. Haruta, D. Kan and Y. Shimakawa, Ferroelectric freestanding hafnia membranes with metastable rhombohedral structure down to 1-nm-thick, *Nat. Commun.*, 2024, **15**(1), 4789.

75 H. Zhang, M. C. Nagashree, R. F. Webster, Z. Wang, X. Zheng, S. D. Kulkarni, R. B. Venkataramana, J. Seidel and P. Sharma, Optical Control of Ferroelectric Imprint in $BiFeO_3$, *Adv. Funct. Mater.*, 2025, 2502700.

